139 (2022) 213022

Contents lists available at ScienceDirect

Biomaterials Advances

journal homepage: www.journals.elsevier.com/materials-science-and-engineering-c

Bioinspired *in vitro* intestinal mucus model for 3D-dynamic culture of bacteria

Lorenzo Sardelli [a,*], Francesco Briatico Vangosa [a], Marta Merli [a], Anna Ziccarelli [a], Sonja Visentin [b], Livia Visai [c,d], Paola Petrini [a]

[a] Department of Chemistry, Materials and Chemical Engineering "Giulio Natta", Politecnico di Milano, Milan, Italy
[b] Molecular Biotechnology and Health Sciences Department, University of Torino, Torino, Italy
[c] Molecular Medicine Department (DMM), Center for Health Technologies (CHT), UdR INSTM, University of Pavia, Pavia, Italy
[d] Department of Occupational Medicine, Toxicology and Environmental Risks, Istituti Clinici Scientifici (ICS) Maugeri, IRCCS, Pavia, Italy

ARTICLE INFO

Keywords:
Microbiota
Gut-on-chip
Rheology
Alginate
Shear rate
E. coli
Gut
bacteria incapsulation
Dynamic culture
Mesh size

ABSTRACT

The intestinal mucus is a biological barrier that supports the intestinal microbiota growth and filters molecules. To perform these functions, mucus possesses optimized microstructure and viscoelastic properties and it is steadily replenished thus flowing along the gut. The available *in vitro* intestinal mucus models are useful tools in investigating the microbiota-human cells interaction, and are used as matrices for bacterial culture or as static component of microfluidic devices like gut-on-chips. The aim of this work is to engineer an *in vitro* mucus models (I-Bac3Gel) addressing in a single system physiological viscoelastic properties (*i.e.*, 2–200 Pa), 3D structure and suitability for dynamic bacterial culture. Homogeneously crosslinked alginate hydrogels are optimized in composition to obtain target viscoelastic and microstructural properties. Then, rheological tests are exploited to assess *a priori* the hydrogels capability to withstand the flow dynamic condition. We experimentally assess the suitability of I-Bac3Gels in the evolving field of microfluidics by applying a dynamic flow to a bacterial-loaded mucus model and by monitoring *E. coli* growth and survival. The engineered models represent a step forward in the modelling of the mucus, since they can answer to different urgent needs such as a 3D structure, bioinspired properties and compatibility with dynamic system.

1. Introduction

The intestinal mucus is a biological hydrogel with heterogeneous and complex functions [1]. Among these, mucus hosts an overwhelming assortment of microorganisms, collectively named gut microbiota [2], in a mutually beneficial relationship with human cells [3]. This coexistence is the result of an evolutionary chain that led the human mucus to be made of two distinct layers: one adherent to the epithelium (attached layer) and one not adherent (loose layer). Chemical compositions, viscoelastic properties and mesh size of the mucus is optimized so that the microbiota is hosted only in the loose one, while the attached one is completely devoid of bacteria [4–10].

The loose mucus layer is transported by the migrating motor complex and peristalsis [11]. This dynamics influences the bacterial gene expression, adhesion to substrate and molecules production [12], resulting, at the macroscopic scale, in changes in growth rate, clearance [13] and intestinal biofilm formation [14]. The dynamic stimuli to which bacteria are physiologically subjected *in vivo* may not be a simple consequence of intestinal motility for nutritive purposes, but the intriguing result of a not-already-described control mechanism on the microbiota biodiversity performed by our body *via* enteric nervous system [15,16]. Thus, the physico-mechanical environment is of top relevance on microbiota characteristics.

Symmetrically, the bacterial presence influences the mucus properties. *In vitro* studies demonstrated, for instance, that mucus permeability increases with overabundance of *Proteobacteria* and *Saccharibacteria* phyla [17]. Similarly, pathogens such as *H. pylori* actively decrease the consistency of the mucins network thus swimming freely towards the mucosa, triggering epithelium infection [18–20].

On the overall, this two-way influence, mucus-to-bacteria and bacteria-to-mucus, has a great relevance to the study how the microbiota affects health and diseases [21]. The *in vitro* study of this interaction is still an open challenge.

Microfluidic systems, like gut-on-chips, are potentially able to

* Corresponding author.
E-mail address: lorenzo.sardelli@polimi.it (L. Sardelli).

https://doi.org/10.1016/j.bioadv.2022.213022
Received 8 January 2022; Received in revised form 27 May 2022; Accepted 5 July 2022
Available online 8 July 2022

reproduce the *in vivo* dynamic environment while sustaining bacterial growth. However, differently from the *in vivo* situation, the intestinal mucus used in dynamic culture is derived from cultured cells or modelled by mucin-based beads or films [22–24]. The chemical interaction can be reproduced by providing mucus components such as mucins. In this cases, the dynamicity is related to the medium flow [11,25,26].

Our ultimate goal is to provide a model with dynamicity mimicking the turnover of intestinal mucus loose layer in a perfused model system. In this case, the dynamicity is not intended as medium flow, but mucus flow. Indeed, we propose a model being an active-dynamic element moving/flowing into channels compatible with microfluidic devices.

Similarly for what is done for cell cultures [27–29], 3D matrices of different materials were used to modulate the bacteria behaviour as an alternative of in suspension cultures in a liquid medium (*i.e.*, planktonic condition) or on 2D growth in agar plates [30–43].

However, these substrates were not aimed to model the viscoelastic properties of mucus. On the other side, few works focused on the optimization of viscoelastic properties of the hydrogels towards the intestinal mucus ones, although not used for either static or dynamic bacterial cultures [44–46].

The chemical composition of the developed mucus models is controlled by standard culture mediums that are used in a wide spectrum of microbiological and cellular applications: LB as typical culture medium for *E. coli*, MH as a reference for antibiotic susceptibility analysis and DMEM as a medium used in cell-bacterial culture in microfluidic systems. We report the combined effect of different 3D environments, containing different culture media, and their effect on the viability and the spatial organization of *E. coli*. This bacterium was selected as it is a commensal bacterium of the human microbiota, particularly studied when investigating the effects of mucus on the bacterial behaviour (and *vice versa*), and for its relevance not only in physiological but also pathological scenario [47–50]. The culture of pathological and commensal strains of *E. coli* was previously studied in *ex vivo* diluted mucus model, without including the complexity and costs deriving from the use of the whole animal [51]. In our study, two different ways to colonize the mucus models are presented: bacteria inoculated on the top of the matrix and the embedding of the bacteria within the matrix to evaluate their migration and viability in the outer layer of the loose mucus. The embedded bacteria can represent a model of the commensal microbial community while the bacteria inoculated on the top of the matrix represent the pathological penetration of pathological strains, where *E. coli* is one of the players involved in both situations. Finally, we discuss how bacterial growth affects the rheological properties of the mucus models.

2. Materials and methods

2.1. Materials

For the I-Bac3Gels preparation: alginate powder (Sigma-Aldrich 180947; Lot MKCG6779), calcium carbonate ($CaCO_3$) (Caelo ph 9.0 Lot 18057507), D-(+)-gluconic acid δ-lactone (GDL) (Sigma-Aldrich G4760; Lot SLBM7762V); medium: Dulbecco's Modified Eagle Medium (DMEM) (EuroClone ECM0101L; Lot EU M035455), Luria Bertani Broth (LB) (Formedium LMM0 102; Lot FMDA114005176); Muller Hinton broth (MH) (Sigma-Aldrich 70,192; Lot BCB275334). The materials used for microbiology were Agar (Formedium™, Lot12/MFM/113), sodium citrate (Sigma Aldrich, Lot BCBW9965) and carbenicillin (CAS#: 4697-36-3).

2.2. I-Bac3Gels preparation

The alginate powder was dissolved in the solvent (DMEM, LB or MH) by gently stirring for at least 12 h. After a process of preliminary optimization, the mass of alginate was defined thus reaching the final concentration of 1 or 2 % (*w/v*) to reproduce the rheological features of the mucus loose layer. Then, a three-dilution process was performed to induce alginate crosslinking. The alginate solution was mixed with fresh medium and a 0.7 % (*w/v*) $CaCO_3$ suspension in a volume ratio of 1:4 (first dilution) and of 1:5 (second dilution). The third dilution consisted in the mixing of the alginate-$CaCO_3$ suspension with a 7 % (*w/v*) GDL solution. Immediately after preparation, the I-Bac3Gels were poured in the proper multiwell plate and stored in fridge for 24 h (4 °C) until use. For sake of simplicity, the name of the mucus models was abbreviated as follow: D-, L- or M- (for DMEM, LB and MH respectively) I-Bac3Gel X% (where X is the alginate concentration, *w/v*, in the model).

2.3. Stability assessment

I-Bac3Gels (664 μL) were poured in a Transwell insert (polycarbonate membrane with 0.4 μm porosity) of a 24-wellplate to obtain 2 mm thick samples stored in fridge at 4 °C. After 24 h, 664 μL of medium (DMEM, LB and MH respectively for D-, L- or M-I-Bac3Gels) were poured in the basolateral chamber of the wells so that I-Bac3Gels were always in contact with the medium and then placed in incubator at 37 °C for the whole stability assessment. Starting from the t_0 (selected as 24 h after I-Bac3Gels production), the samples were dried for 10 s, to remove the liquid excess, and weighted at different time points: 15 min, 30 min, 1 h, 2 h, 4 h, 24 h, 48 h and 72 h. After 72 h, the samples weight was measured each week up to 21 days and normalized with reference to the initial weight (w(%) at t_0 equals to 100 %). Stability was assessed accordingly to the formula (Eq. (1))

$$w(\%) = \left(1 + \frac{w(t) - w(t_0)}{w(t_0)}\right) \bullet 100 \quad (1)$$

2.4. Rheological characterization

Viscoelastic properties of I-Bac3Gels were investigated using a rotational rheometer (Anton Paar, Modular Compact Rheometer MCR 502) in a strain-controlled configuration with parallel plates geometry (25 mm diameter) (Anton Paar, serial number: 52890). The temperature and the gap between plates were set at 25 °C and 0.5 mm, respectively, for all the experiments. The I-Bac3Gels properties in oscillatory regime were characterized in terms of Storage (G', Pa) and Loss (G'', Pa) moduli, which indicate the material capability of elastically store and viscously dissipate energy, respectively. Increasing values of shear strain, from 0.01 % to 1000 %, were applied to I-Bac3Gels after 24 h from preparation to identify the linear viscoelastic region (LVR) at 1.0 Hz. According to the LVR results, a 0.5 % oscillating strain amplitude (at 1.0 Hz) was applied for 2 h to identify the nominal gel-points. Then, the viscoelastic behaviour in dependence of frequency (from 0.1 Hz to 20 Hz) was obtained by frequency sweep test at the fixed shear strain of 0.5 % performed 24 h after preparation. For I-Bac3Gels 1 %, frequency sweep tests were also performed in the same experimental set up but 5 h after preparation to investigate the viscoelastic properties of the I-Bac3Gels in a time comparable to the *E. coli* dynamic culture one (see paragraph 2.7.2.3).

2.5. Extrudability characterization

The extrudability of the I-Bac3Gels was investigated *via* shear rate ramp (from 0.1 to 100 s^{-1}) in a steady state rotation experiment and shear stress ramps (from 0.1 to 100 Pa) in an oscillatory experiment performed at 1.0 Hz after 24 h from preparation. The latter experiment aimed at estimating the gel yield stress, while the former at determining the viscosity curve and the power law index of its interpolation *via* a power law. For the sake of simplicity this index will be taken as the only significant parameter for the description of the system flow, and will be referred to as flow-behaviour index in this paper. For i-Bac3gel 1 %, the flow-behaviour index and the yield stress were also evaluated after 5 h

(time of the *E. coli* dynamic culture) from preparation by maintaining the same experimental set-up used for completed crosslinked models (24 h). The dynamic stimulation on I-Bac3Gels was performed by connecting 10 ml Terumo luer-lock syringes filled with hydrogel to a ~ 15 cm silicon tubes (i.d. of 1.58 mm) after 24 h from preparation. Each tube was fixed to a 35 mm petri dish, which acted as reservoir of the extruded samples. The I-Bac3Gels were extruded at different flow rates (0.5, 1 and 5 μL/min) by syringe pump (Harvard Apparatus PHD ULTRA) and characterized by frequency sweep test after extrusion. For 1 % I-Bac3-Gels, the dynamic extrusion was also performed immediately after preparation, extruding the hydrogels at 1 μL/min, which is the flow rate used for *E. coli* dynamic culture.

2.6. Characterization of the I-Bac3Gels internal microstructure

The data of the frequency sweep tests were analyzed by means of the Generalized Maxwell Model (GMM). The GMM is a parallel of n Maxwell-elements, each one consisting of a series of spring (with specific modulus G_i) and a dashpot (with specific viscosity, η_i), which model the elastic and viscous components of a viscoelastic material. Each element is characterized by a relaxation time, $\lambda_i = \eta_i/G_i$, A further pure elastic element (spring with a modulus G_e) is inserted in parallel to the other n elements. GMM can be exploited to obtain a theoretical form of G' (Eq. (2)) and G'' (Eq. (3)) in function of the pulsation ω:

$$G' = G_e + \sum_{i=1}^{n} G_i \frac{(\lambda_i \omega)^2}{1 + (\lambda_i \omega)^2}; G_i = \frac{\eta_i}{\lambda_i} \quad (2)$$

$$G'' = \sum_{i=1}^{n} G_i \frac{\lambda_i \omega}{1 + (\lambda_i \omega)^2}; G_i = \frac{\eta_i}{\lambda_i} \quad (3)$$

The relaxation times are assumed not to be independent of each other, but scaled by a factor 10 as reported in other works [52,53]. The number of elements was chosen thus minimizing $\chi^2 \bullet Np$, where Np (=2 + n) is the number of fitting elements and χ^2 is the chi-square error.

The frequency response of the I-Bac3Gels viscoelastic properties (G' and G'' measured as described in paragraph 2.4) were fitted by using 1- to 10-elements Generalized Maxwell Models (GMM). To this aim, a specific MATLAB function was implemented. The GMM fitting was used to obtain the shear modulus of the I-Bac3Gels by means of Eq. (4):

$$G_\infty = G_e + \sum_{i}^{n} G_i \quad (4)$$

where G_∞ [Pa] is the shear modulus for the material when any relaxation phenomenon was over, defined as the ratio between the shear stress and the shear strain. The G_∞ of all I-Bac3Gels was then interpreted in the view of the rubber elasticity theory. This allowed to estimate the number (per unit volume) of the elastically active polymeric chains, ρ, by using the Eq. (5):

$$\rho = \frac{G_\infty}{R\,T} \quad (5)$$

where R is the universal gas constant and T the absolute temperature. In order to estimate the average mesh size (ξ), the equivalent network theory is used and another assumption is made: the real network topology is substituted by an idealized one with same ρ. In particular, the idealized topology consists in a network with dimension that can be modelled as made by a collection of identical spheres centred in each crosslinking-sites. With this hypothesis, the relation between ξ and ρ is:

$$\xi = \sqrt[3]{\frac{6\rho RT}{\pi N_A G}} \quad (6)$$

where N_A is the Avogadro's number.

2.7. Characterization of bacteria viability in I-Bac3Gels

2.7.1. E.coli culture conditions

Non-pathogenic *E. coli* strain (ATCC 25922) was cultured in 10 ml of medium (DMEM, LB or MH) and incubated at 37 °C o/n. The OD_{600} of the resulting bacteria suspension was measured by a spectrophotometer (Aurogene, UV-VIS Spectrophotometer HJ908003) and converted in bacteria concentration (#bacteria/ml) by using a standard calibration curve of bacterial growth. The inoculum was then diluted accordingly to the necessities for the type of infection.

2.7.2. I-Bac3Gels infection with E. coli

I-Bac3Gels infection was performed in 3 different experimental conditions as follows.

2.7.2.1. External infection of I-Bac3Gels with E. coli. Immediately after preparation, 100 μL of I-Bac3Gels were poured in well of commercial sterile 96-wells plate. After 24 h, 100 μL of an *E. coli* suspension, at the concentration of $5 \bullet 10^4$ bacteria/ml, was transferred on the top of I-Bac3Gels thus infecting the hydrogels. The externally infected I-Bac3-Gels were incubated at 37 °C for 24 h.

2.7.2.2. Internal infection of I-Bac3Gels with E. coli. For internally infected I-Bac3Gels, the preparation process of the hydrogels was modified as follow: the alginate solution was mixed with an *E. coli* suspension in a volume ratio of 1:4 (first dilution). A 0.7 % (*w/v*) $CaCO_3$ suspension and 7 % (w/v) GDL solution were mixed in series to the infected alginate solution in a volume ratio of 1:5 and 1:6, respectively (second and third dilutions). The initial bacterial suspension was set to reach a final concentration of $5 \bullet 10^4$ bacteria/ml. Immediately after preparation, 100 μL of internally infected I-Bac3Gels were deposited in a well of a sterile commercial 96-wells plate. After 5 h, 100 μL of fresh medium were dispensed on the samples to provide renewal of nutrients. The internal infected I-Bac3Gels were incubated at 37 °C for 24 h.

2.7.2.3. Dynamic stimulation of internally infected I-Bac3Gels. Internally infected I-Bac3Gels were prepared as reported above (Section 2.7.2.2). Then, 2 ml of infected I-Bac3Gels (bacteria concentration of $5 \bullet 10^4$ bacteria/ml) were placed in a 10 ml Terumo luer lock syringe and connected to a 35 mm petri dish (reservoir) by ~ 15 cm silicon tube with an inner diameter of 1.58 mm. The internally infected I-Bac3Gels were then extruded with a flow rate of 1 μL/min for 5 h maintaining the temperature at 37 °C.

2.7.3. Colony forming units (CFU) assay for assessment of E. coli viability

The assessment of *E. coli* viability was performed by CFUs counting on LB-agar plates (2.5 % (*w/v*) LB culture medium containing 1.5 % (w/v) agar, Difco).

As previously indicated, after 24 h of infection, the supernatant of the externally infected I-Bac3Gels was removed, serially diluted and plated on LB-agar plates for CFU counting. The I-Bac3Gels infected in external, internal or dynamical stimulated conditions were washed three times with 100 μL of fresh medium to remove non-adherent bacteria. The I-Bac3Gels were then treated with 150 μL of 50 mM sodium citrate solutions to trigger hydrogels destruction while not damaging bacterial cells. After homogenization and serial dilution, 10 μL of dissolved I-Bac3Gels were plated in duplicates on the LB-agar plates and incubated at 37 °C o/n. The CFUs were manually counted after 24 h.

2.8. Confocal laser microscopy for the evaluation of E. coli distribution

2.8.1. GFP-expressing E. coli transformation

To express a GFP-fluorescent strain, E.coli strain (ATCC 25922) was transformed by electroporation with a pMF230 DNA plasmid as previously showed [54]. Briefly, *E.coli* was electroporated by serial dilution in

electroporation buffer (10 % sterile glycerol solution, kept at −20 °C) from an exponential phase overnight culture (OD_{600} = 0.6) in LB medium. The bacterial overnight culture was pelleted and re-suspended in the electroporation buffer. Then, the bacterial suspension was centrifuged and re-suspended in half the initial culture volume with fresh electroporation buffer. This process was repeated until the volume was reduced to 0.01 of the initial volume. The electrocompetent cells were used within 1 h after preparation or stored at −80 °C immediately after preparation in aliquots of 70 μL.

The pMF230 plasmid DNA was acquired from the Addgene database as a bacterial stab of *E. coli* DH5α. To produce plasmid DNA for *E.coli* transformation, *E. coli* DH5α was grown overnight in LB with 300 μg/mL carbenicillin (CB, Sigma). The pMF230 plasmid DNA was extracted using QIAprep Spin Miniprep kit (Quiagen) according to manufacturer instructions. After extraction, the pMF230 plasmid DNA was diluted in sterile deionized water to reach concentrations between 0.1 and 1 μg/mL.

To transfer the exogenous DNA, 80 μL of electrocompetent *E.coli* suspension was mixed with 1 μg of pMF230 plasmid DNA and this suspension was kept in ice for 30 min before electroporation. The electroporation process was conducted in a Gene Pulser Electroporation system (BioRad, USA), using a conductive cuvette. The electric pulse was given for 5 ms at 2.5 kV, 200 Ω, 25 μF. After the shock, the content of the cuvette was transferred to a falcon tube, containing 1 mL of SOC medium (2.0 % Tryptone, 0,5 % Yeast Extract, 10 mM NaCl, 2,5 mM KCl, 10 mM MgCl2, 10 mM MgSO4 and 20 mM D-glucose) left in incubation under shaking conditions for 2 h at 37 °C. Upon 2 h of recovery, the suspension was plated on LB agar plates containing 300 μg/mL carbenicillin. Agar plates single colonies were grown overnight in LB containing 300 μg/mL carbenicillin at 37 °C and glycerol stocks of GFP-*E. coli* were kept at −80 °C immediately after preparation.

2.8.2. Evaluation of the E. coli distribution in I-Bac3Gel

For the maintaining the GFP-expressing plasmid, 300 ng/ml of carbenicillin were diluted into either the inoculum used for the infections and the alginate solution for the I-Bac3Gels preparation.

Both externally and internally infected I-Bac3Gels were placed into 35 mm petri dishes in a final volume of 2 ml. Then, sections of the I-Bac3Gels with fluorescent *E. coli* were observed after 24 h by a modular confocal microscope (Leica TCS SP8 Lighting) with a magnification of 40×. Analyses were performed at a wavelength of 488 nm (EX/EM maxima ~500/550).

As a control, I-Bac3Gels without bacteria was observed under confocal microscopy at the aforementioned wavelength to evaluate the absence of possible autofluorescence effects.

2.9. Rheological characterization of I-Bac3Gels infected by E. coli

Bac3gels (2 ml) were placed in petri dishes with 35 mm of diameter. In case of external infection, 2 ml of *E. coli* at the concentration of $5\bullet10^4$ bacteria/ml were poured after 24 h from the preparation on the top of I-Bac3Gels. In case of internal infection, 2 ml of fresh medium was added after 5 h from the sample preparation. After 24 h from infection, the supernatant was removed, and the samples were further washed 3 times with 2 ml of fresh medium. Then, infected I-Bac3Gels were allocated between the two plates of the rheometer for the measurements. Frequency sweep test was performed to evaluate the changes in the viscoelastic properties (G' and G'') induced by infection maintaining the same experimental parameters of sterile I-Bac3Gels rheological characterization.

2.10. Statistical analysis

The results are shown with mean ± standard deviation (SD) computed for at least four repetitions. D'Agostino-Pearson test was used to investigate the normality of the data distribution. Then, ANOVA or Kruskal-Wallis tests were used to compare groups of data. The statistical analysis was performed by using GraphPad Prism 9 (GraphPad Software, USA). Differences were represented in the graphs only when statistically significant. Differences were considered statistically significant in case of $p < 0.05$ (*), $p < 0.01$ (**), $p < 0.001$ (***) and $p < 0.001$ (****).

3. Result

The I-Bac3Gels showed shape-maintenance capability and transparent appearance, independently from alginate concentration and medium type, but different colours. Indeed, D-I-Bac3Gel was characterized by a saturated pink colour, while L-I-Bac3Gel showed a yellow shaded tint and M-I-Bac3Gel was colourless (Fig. 1).

3.1. Stability assessment

The stability of I-Bac3Gels was tested in a period of 21 days (Fig. 1). The variation of weight was <10 %, with a maximum weight loss of 9.8 ± 2.1 % for M-I-Bac3Gel 1 % (Fig. 1-C). Alginate concentration did not appear to play a role in the stability of I-Bac3Gel, as well as the medium type used for their production.

3.2. Rheological characterization

The LVR was identified as the maximum shear strain amplitude after which the storage and loss started changing from the previous constant value. The I-Bac3Gels exhibited the typical gel-like behaviour ($G' > G''$, $\tan(\delta) < 1$) independently from medium type, with an LVR correlated to the alginate concentration (S.I. Table 1). Indeed, the LVR of D- and L-I-Bac3Gel was indirectly proportional to the alginate content, while the LVR of M-I-Bac3Gel was found proportional to alginate concentration. In the view of these results, a shear strain of amplitude 0.5 % was chosen as input for further rheological characterizations.

The nominal gel point, which was here selected as the moment when the storage modulus equals the loss modulus, was identified for all the medium types and alginate concentration of 1 % and 2 % (Table 1). Even if the gel points were reached before 1 h for each I-Bac3Gel, in D-I-Bac3Gel the polymeric network formed faster than in the two other I-Bac3Gels types. Indeed, the nominal gel point of D-I-Bac3Gels was about half of the other two gel points. Moreover, the $G' - G''$ measured after 5 h (S.I. Fig. 1 A) showed that the D-I-Bac3Gel 1 % gained ~ 64 % of its final G' value (87 % in case of G'') in 21 % of the whole crosslinking time considered (24 h). Differently, L- and M- I-Bac3Gels 1 % were able to reach only the 22 and 6 % of their final G' values, respectively, (17 and 4 % for G''). This trend was also confirmed for models with 2 % of alginate (Fig. S.I. B).

After 24 h from preparation, the I-Bac3Gels exhibited gel-like behaviour with the elastic contribution exceeding the viscous contribution within the frequency range considered (Fig. 2 A-B-C). The G' and G'' of I-Bac3Gels were dependent from the solvent considered at the relevant frequencies of the migrating motor complex and typical bacterial motion (0.1 and 1.0 Hz respectively) [11,55]. Indeed, the viscoelastic properties of M-I-Bac3Gels exceeded those of D- and L-I-Bac3Gel for both 1 and 2 % alginate. The alginate concentration had effect on the G' and G'' in case of D- and L-I-Bac3Gels, with enhanced viscoelastic properties in case of 2 % (*w/v*) alginate content (Fig. 2 D, E and G, H). For instance, the G' increases of 55 and 47 % for D- and L-I-Bac3Gels, respectively (71 and 56 % if G'' is considered). Differently the alginate concentration did not impact significantly the viscoelastic properties of M-I-Bac3Gels (Fig. 2 F and I).

3.3. Flowability characterization

The viscosity curves were comparable for mucus models obtained with different media, iand at the same alginate concentration (Fig. 3). However, an increasing polymer content from 1 % to 2 % induced higher

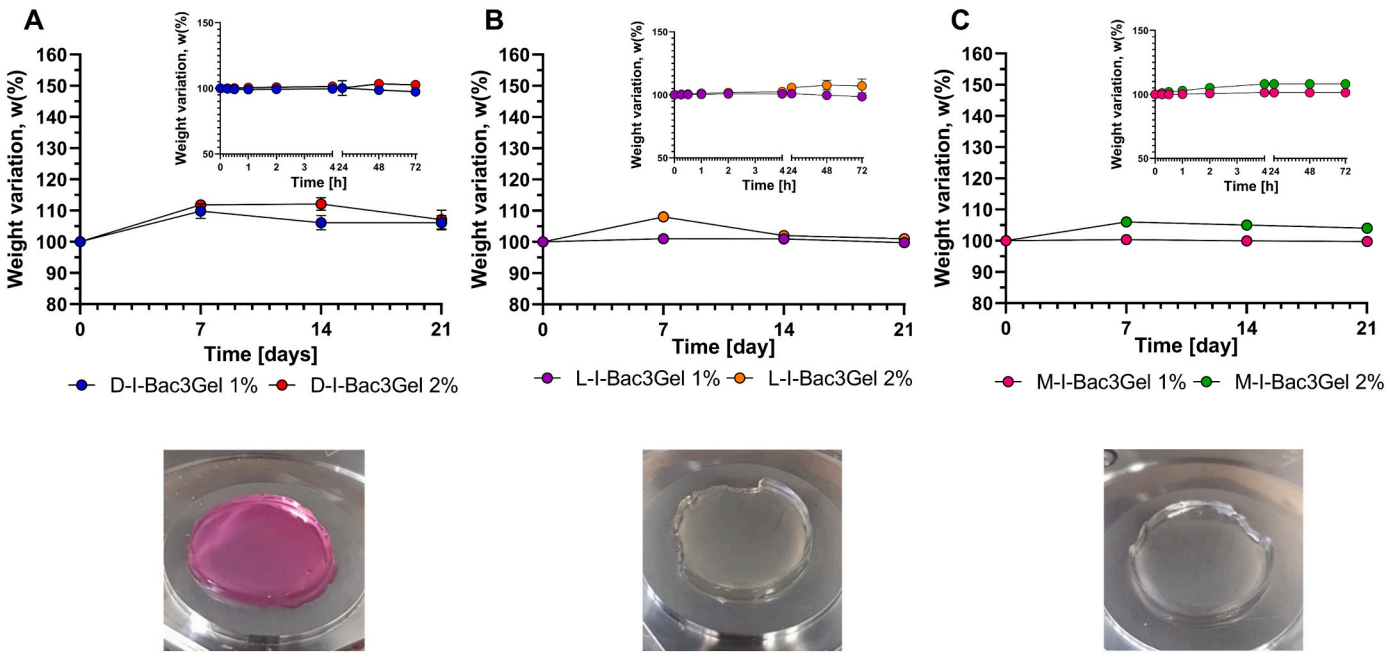

Fig. 1. Stability assessment of the D-I-Bac3Gel (A), L-I-Bac3Gel (B) and M-I-Bac3Gel for 21 days. The insets showed the stability for the time points considered before 72 h. The pictures below the stability plots showed a representative image of the respective mucus models.

Table 1
Gel point, yield stress and flow behaviour index measured for the I-Bac3Gels 1 % and 2 % obtained with different mediums.

		gel point (min)	Yield Stress (Pa)	n
I-Bac3Gels 1 %	DMEM	23 ± 5	16 ± 4	0.39 ± 0.11
	LB	52 ± 8	15 ± 3	0.36 ± 0.10
	MH	43 ± 7	10 ± 3	0.39 ± 0.05
I-Bac3Gels 2 %	DMEM	31 ± 11	35 ± 7	0.28 ± 0.06
	LB	48 ± 7	21 ± 4	0.19 ± 0.03
	MH	36 ± 4	48 ± 5	0.25 ± 0.11

viscosity values. Indeed, at the minimum considered shear rate (0.1 s^{-1}) the viscosity increased by a factor of 2,3 and 4 in case of D-, L- and M-I-Bac3Gel (Fig. 3 A-B and C, respectively). The viscosity curves were interpreted in the view of the power law equation (Eq. (7)), which describes the relationship between viscosity and the shear rate in the form:

$$\eta = K(\dot{\gamma})^{n-1} \quad (7)$$

where η is the viscosity, K the flow consistency index, $\dot{\gamma}$ the shear rate and n the power law index. This parameter was lower than one for all the I-Bac3Gels (Table 1), with minimum value obtained for the L-I-Bac3Gels 2 % and maximum for D-I-Bac3Gels 1 %.

Similarly, the viscosity curve of I-Bac3Gels 1 % showed a shear thinning behaviour when measured at 5 h after production (S.I. Fig. 2 A) independently from the medium used for the hydrogels production. Although the viscosity values were found comparable with those of I-Bac3Gels tested after 24 h from production (~99 % of the final values), the flow behaviour index was found to be lower than that of completely formed I-Bac3Gels (24 h after preparation). Indeed, n was equal to 0.23 ± 0.11, 0.21 ± 0.09 and 0.20 ± 0.10 for D-, L- and M-I-Bac3Gels 1 % respectively.

The yield stress was identified as the shear stress amplitude at which the viscoelastic properties of I-Bac3Gels passed from a gel-*like* to a liquid-*like* material (*i.e.*, from tan(δ) < 1 to tan(δ) > 1) (Fig. 3 D, E and F). A yield stress was identified for I-Bac3Gels characterized after 24 h from preparation, independently form the type of medium and alginate content, as the tan(δ) curves intersected the unit value in the range of oscillatory shear stress range considered (Table 1). The yield stress values were directly proportional to alginate concentration, with the I-Bac3Gels 1 % characterized by lower shear stress than I-Bac3Gels 2 % for each medium type (Fig. 3 D, E and F). The medium did not affect the yield stress in case of alginate 1 %, which varied from 10 ± 3 to 16 ± 4 Pa in case of M- and D-I-Bac3Gels, respectively (Fig. 3 F and D, respectively). Differently, the medium used for the production influenced the yield values of I-Bac3Gels with 2 % alginate content, which was maximum in case of M-I-Bac3Gel (48 ± 5 Pa), intermediate in case of D-I-Bac3Gel (35 ± 7 Pa) and minimum in case of L-I-Bac3Gels (21 ± 4 Pa).

The presence of a yield stress was also confirmed after 5 h from preparation for the I-Bac3Gels 1 % (S.I. Fig. 2 B). Indeed, the tan(δ) passed from lower to higher values than the unit in the considered range of shear stress amplitudes. The independence of yield stress from medium was confirmed also in this case, as the yield stress varied from 10 ± 4 to 16 ± 4 Pa (D- and M-I-Bac3Gels 1 % respectively) with values comparable with the ones found after 24 h from production.

The suitability of I-Bac3Gels for dynamic culture of bacteria was assessed by dynamically extruding the mucus models by syringe pumps. The frequency dependence of the I-Bac3Gels viscoelastic properties were evaluated in function of the applied flow rates used to extrude the hydrogels from the syringes. Interestingly, the dynamic stimulation did not influence the properties of the I-Bac3Gels, which maintained the gel-*like* characteristics ($G' > G''$, $tan(\delta) < 1$) in the range of frequency considered (Fig. 4). Moreover, the viscoelastic properties did not change significantly from the static condition, at the relevant frequencies of 0.1 and 1.0 Hz (*i.e.*, migrating motor complex and bacterial motion), apart from D-I-Bac3Gels 1 %. In this case, an increase of both G' and G'' was observed when the highest flow rate (5 μL/min) was used to extrude the model (Fig. 4 A-B).

The viscoelastic properties of I-Bac3Gels 1 % extruded at 1 μL/min immediately after production were analyzed as soon as sufficient material was collected in the reservoir (5 h after preparation, time comparable to the bacterial dynamic culture as reported in paragraph 2.7.2.3). Indeed, no statistical differences were found between immediately extruded I-Bac3Gels 1 % and static control, with G' values of 40 ± 8 Pa for D-I-Bac3Gels and 10 ± 1 Pa for L- and M-I-Bac3Gels (S.I.

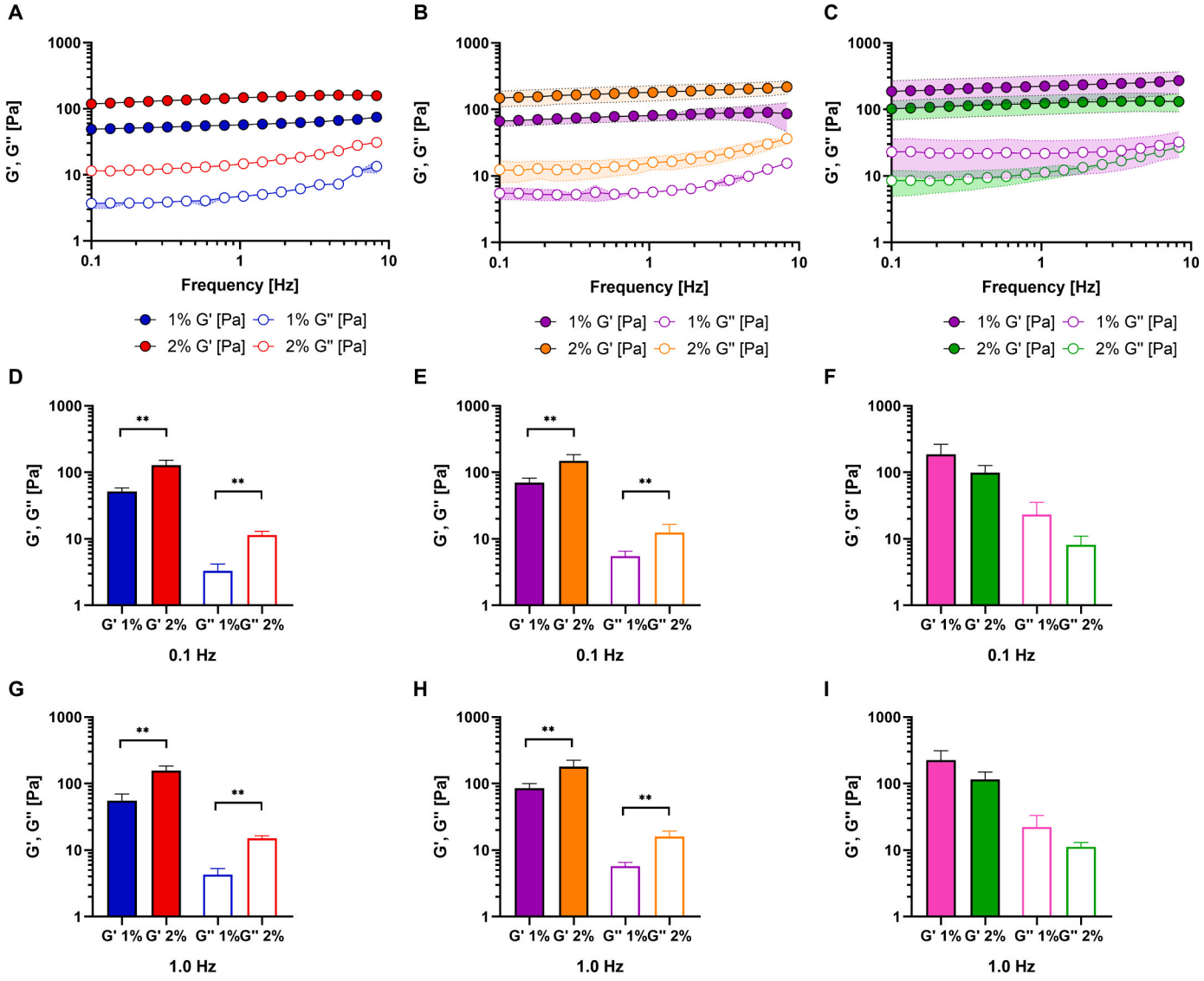

Fig. 2. Frequency response of the D-, L- and M-I-Bac3Gels (A, B and C, respectively) and viscoelastic properties extracted at the relevant frequencies of the migrating motor complex (0.1 Hz) and bacterial motion (1.0 Hz) for D- I-Bac3Gels (D, G) L- I-Bac3Gels (E, H) and M- I-Bac3Gels (F, I).

Fig. 3).

3.4. Characterization of the I-Bac3Gels internal structure

The estimated mesh sizes for D-I-Bac3Gel 1 % (Fig. 5 A) showed a reduction of the network microstructure after extrusion, independently from the flow rates applied (decrease up to 60 %). D-I-Bac3Gel 2 % exhibited lower mesh size than the D-I-Bac3Gel 1 %, with a mesh of 34 ± 5 nm and 42 ± 14 nm, respectively. Similarly to D-I-Bac3Gel 1 %, the extruded D-I-Bac3Gel 2 %, was characterized by a lower mean mesh size than the static condition (Fig. 5 A).

L-I-Bac3Gel 1 % and 2 % showed a similar mesh size independently from the flow used for the extrusion, with the static controls characterized by mesh of 42 ± 5 nm and 34 ± 3 nm, respectively (Fig. 5 B).

M-I-Bac3Gel 1 % exhibited a mesh size before extrusion of 32 ± 5 nm, which was comparable the other hydrogel types. The mesh sizes of M-I-Bac3Gel 1 % showed the maximum decrease when extruded at 5 μL/min (*i.e.*, mesh size of 25 ± 5 nm).

The mesh size before extrusion of M-I-Bac3Gel 2 % was estimated to be 33 ± 3 nm, with a maximum decrease of 5 nm after extrusion at the flow rate of 0.5 μL/min.

3.5. Bacteria viability in I-Bac3Gels

The availability of *E. coli* was investigated in case of external and internal infection of I-Bac3Gels 1 %.

The number of *E. coli* cultured in I-Bac3Gel 1 % was not influenced by the type of infection. The CFU counted in externally and internally infected I-Bac3Gels was comparable for each medium used (Fig. 6 A). Differently, the medium used for the I-Bac3Gels preparation had a role in the final concentration of bacteria. Indeed, in case of external infection, the number of bacteria was maximum in L-I-Bac3Gel 1 % and minimum in D-I-Bac3Gel 1 % ($3{\cdot}10^9$ and $7{\cdot}10^8$ bacteria/mL, respectively). When internal infection is considered, the highest CFUs number was found for M-I-Bac3Gel 1 % ($2{\cdot}10^9$ bacteria/ml), while the minimal concentration was found in D-I-Bac3Gel 1 % ($4{\cdot}10^8$ bacteria/ml). The bacteria availability after 24 h of infection was similar to the number of bacteria cultured in standard suspension methods (*i.e.*, planktonic controls) independently from the type of medium and infection, (with the exception of internally infected L-I-Bac3Gel 1 %) (Fig. 6 A).

To evaluate the intrinsic capability of the I-Bac3Gel itself to sustain the bacterial growth, CFUs counting was performed also without submerging the mucus models in the different media when internal

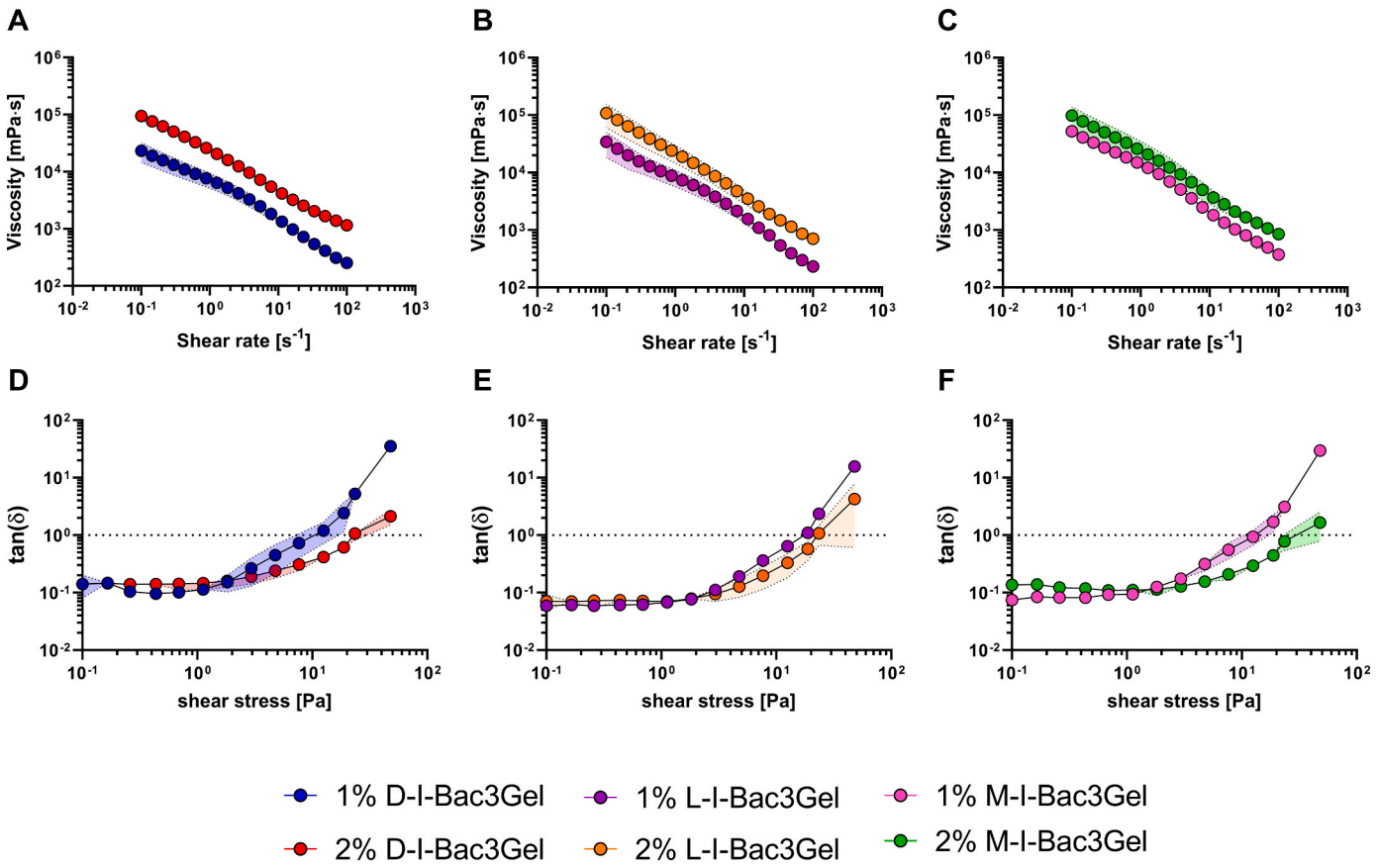

Fig. 3. Extrudability characterization performed by analysing the viscosity profiles of D-, L- and M-I-Bac3Gels 1 and 2 % (A, C and D respectively) and the tan(δ) curves in function of the oscillatory shear stress ramp for I-Bac3Gels 1–2 % (D for D-I-Bac3Gels, E for L-I-Bac3GelS and F for M-I-Bac3Gels).

infection was used. Interestingly, the presence of medium to surrounding the mucus model was not necessary for the bacteria viability, as the CFUs obtained with and without the addition medium to the formed hydrogels were comparable for all types of mucus models (Fig. 6 B).

Finally, the bacteria viability was studied in dynamic culture within the I-Bac3Gels 1 %. The internally infected I-Bac3Gels efficiently supported the bacterial growth during the motion of the models inside the tubes (extrusion duration: 5 h). Indeed, the final CFUs counted in I-Bac3Gels were comparable to the planktonic control for all the mediums considered (Fig. 6 C) and were equal to $5.0 \pm 2.0 \cdot 10^6$, $2 \pm 0.3 \cdot 10^6$ and $2 \pm 0.4 \cdot 10^6$ bacteria/mL for D-, L- and M-I-Bac3Gels respectively.

3.6. Confocal laser microscopy for evaluation of the E. coli distribution

Fluorescent *E. coli* was homogeneously distributed in the whole sections of the I-Bac3Gels, suggesting that the type of infection and culture medium did not influence the distribution of bacteria in the models (Fig. 7). However, either the composition or the type of infection effected the organization of the *E. coli* communities.

Externally infected D-I-Bac3Gel 1 % exhibited bacteria aggregates with a mean length of ~ 100 μm, while the internal infection did not show formation of clusters of appreciable dimensions, even if small aggregates of bacteria may also be seen in this case (Fig. 7). The *E. coli* was homogeneously distributed in both external and internal infected D-I-Bac3Gel. In L-I-Bac3Gel 1 %, *E. coli* was organized in cellular chains independently from the infection strategy (Fig. 7) with a higher bacterial aggregation degree in externally infected L-I-Bac3Gel 1 % compared to the internally ones.

E. coli cultured in M-I-Bac3Gel 1 % exhibited bacillus-*like* appearance without aggregates and was homogeneously distributed in the entire section independently from the type of infection.

3.7. Rheological characterizations of I-Bac3Gels infected by E. coli

The rheological characterization of I-Bac3Gels 1 % with bacteria was evaluated by frequency sweep tests. The presence of bacteria in the mucus models did not impair the formation of a permanent polymeric network, as the elastic contribution (G') was higher than the viscous contribution (G'') for all the I-Bac3Gels 1 % and type of infection. The medium used for the I-Bac3Gels 1 % production greatly influenced the variation induced by bacteria in the viscoelastic properties compared to sterile control. In case of D-I-Bac3Gels, the G' values were comparable between sterile and infected I-Bac3Gels in both internal and external infections (Fig. 8). Differently, the G'' of either external or internal infected D-I-Bac3Gel 1 % increased by a factor of 10.

L-I-Bac3Gel 1 % showed two completely different trends between external and internal infections. In the first case, L-I-Bac3Gel 1 % exhibited an increased storage and loss moduli (*i.e.* they doubled with respect to sterile L-I-Bac3Gel 1 %) (Fig. 8). In the second case, the G' was lower than controls and the G'' increased from lower to higher frequencies showing a significant dependence on frequency (Fig. 8).

The G' of M-I-Bac3Gel 1 % was lower than sterile controls in both external and internal infections, with maximum decrease in the second case. Differently, G'' decreased in case of M-I-Bac3Gel 1 % with embedded *E. coli* while it increased in case of external infection.

4. Discussion

The intestinal mucus is a complex microenvironment that is heavily colonized by billions of microorganism, collectively labelled as microbiota [7–10,17,56–59]. Even if the viscoelastic properties of intestinal mucus influence the microbiota distribution, migration and metabolism, a limited numbers of studies assessed the optimisation of *in vitro* mucus

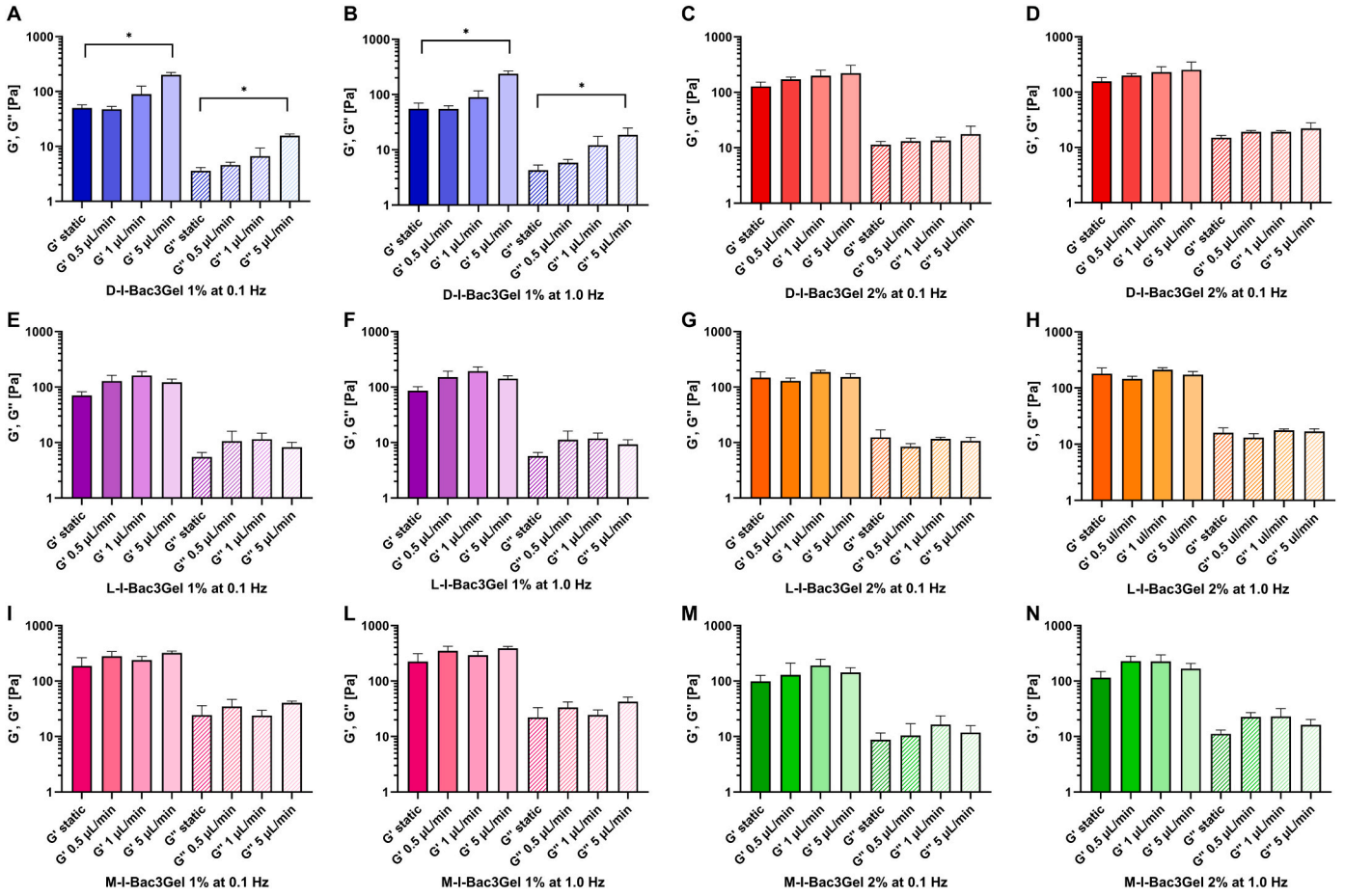

Fig. 4. Effect of the dynamic stimulation performed at different flow rates on the viscoelastic properties, *G'* and *G''*, measured at 0.1 or 1.0 Hz of D-I-Bac3Gel 1 % (A and B) and 2 % (C and D), L-I-Bac3Gel 1 % (E and F) and M-I-Bac3Gel 1 % (I and L) and 2 % (M and N).

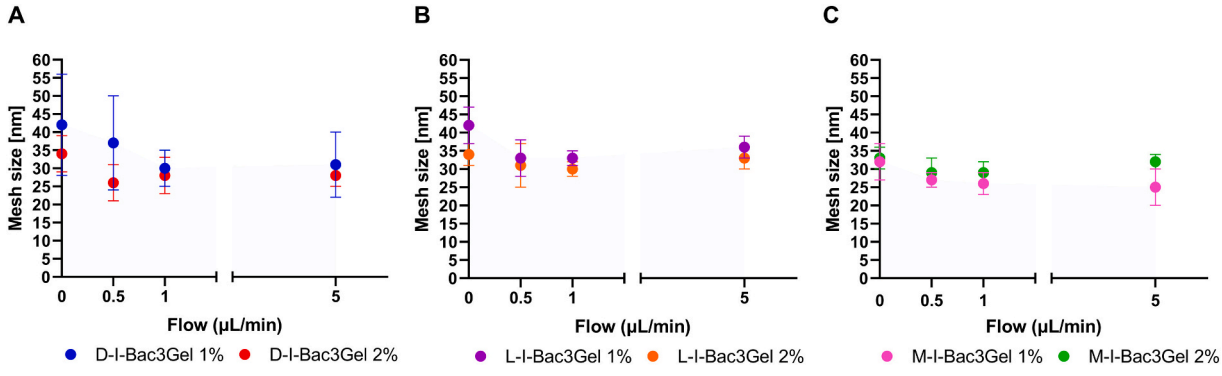

Fig. 5. Mesh size obtained exploiting the GGM in function of the alginate concentration and the flow rate used for the extrusion of D-I-Bac3Gel (A), L-I-Bac3Gel (B) and M-I-Bac3Gel (C) .

models in terms of viscoelasticity [44,60,61].

In this work, a bioinspired mucus model, called I-Bac3Gel, was developed and optimized with viscoelastic properties comparable to the physiological intestinal loose mucus layer (*i.e.*, 2–200 Pa) [62]. The I-Bac3Gels were designed to contain different culture media to fit the model with the proper environment required for the specific culture. This set up adds the possibility to evaluate the effect of a 3D architecture with minor changes in the chemical composition. Therefore, I-Bac3Gel can be considered a solid medium, similarly to what is done with agar for bacterial culture [63]. Alginates undergo ionic crosslinking, which is compatible with protein containing media, such as DMEM, that may undergo protein denaturation during thermal gelation of unmodified agarose [64,65]. Alginate is also considered as an alternative polysaccharide to agarose in specific cases, where solid agar medium may inhibit in a concentration-dependent mechanism the growth or isolation of specific strains of bacteria [63,66,67]. We proved this concept including not only bacterial culture medium (LB and MH), but also a cell culture medium (DMEM). The I-Bac3Gels produced with DMEM, in particular, offers the possibility to use I-Bac3Gel in complex system such as gut-on-chips, where the co-culture of bacteria and cells is a mandatory key point for different fields of interest [23]. The compositional changes imposed by varying the media and alginate concentration were pivotal

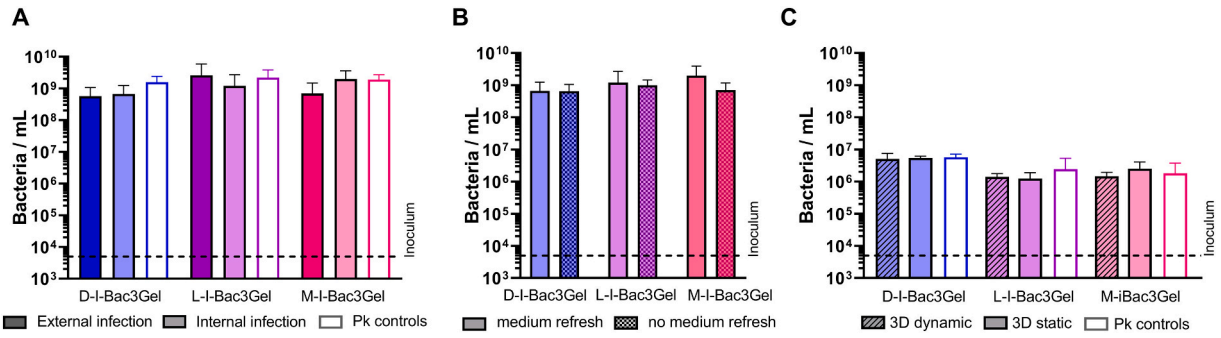

Fig. 6. A) Bacterial concentration in the I-Bac3Gels 1 % obtained with different type of infection in static condition with or without (B) medium refresh. C) Availability of bacteria in I-Bac3Gels at the end of the dynamic stimulation performed with the flow rate of 1.0 μL/min. The differences were found not statistically different ($p > 0.90$).

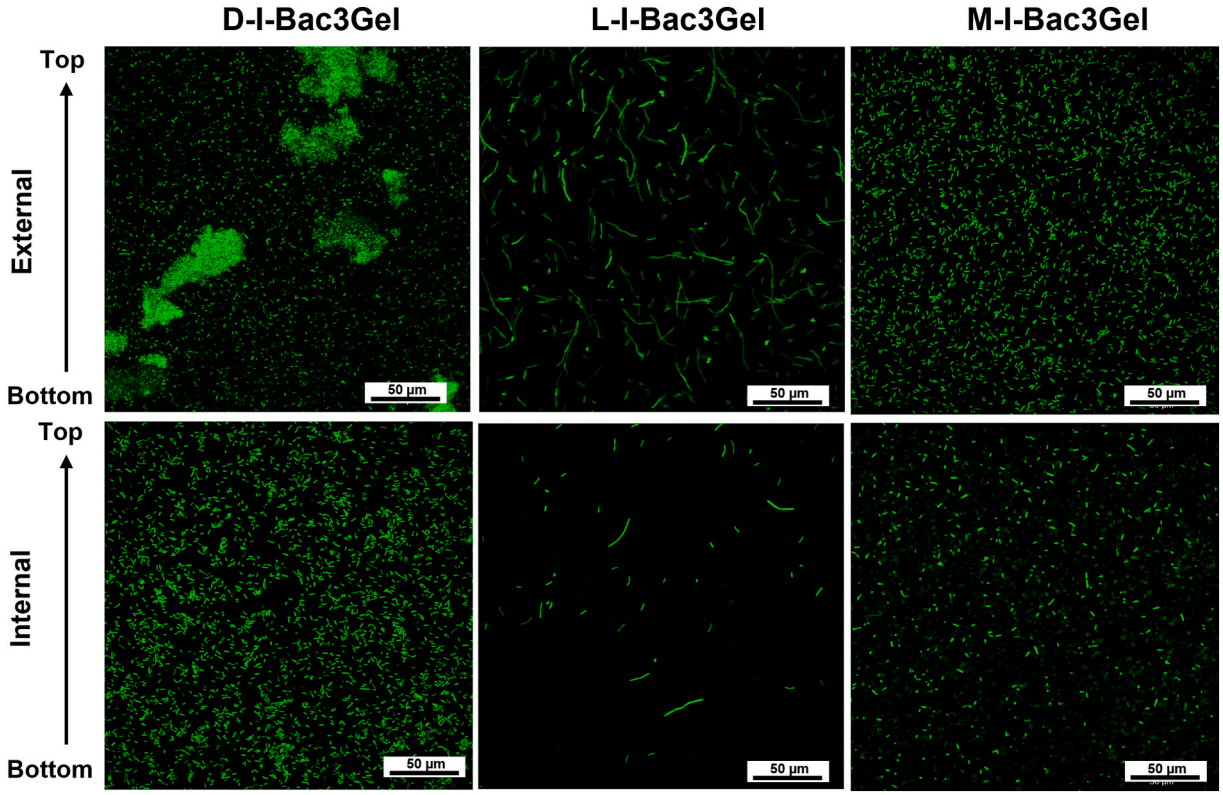

Fig. 7. Confocal laser microscopy images of GFP-expressing *E. coli* observed in section of I-Bac3Gel 1 % infected by either pouring bacteria onto already formed hydrogels (external infection) or by incorporation bacteria during the production process (internal infection). Reference bar of 50 μm.

in the determination of the I-Bac3Gels viscoelastic and structural properties (Fig. 2 and Fig. 5). The composition of the hydrogels did not impact the stability of the models, which remained in the physiological range (*i.e.*, 2–200 Pa) typical of mucus, preserving their shape, size and geometry (Fig. 1, Fig. S.I. 4).

The I-Bac3Gels viscoelastic properties were instead tuned by alginate content. Indeed, the G' and G'' of the models increases increasing polysaccharide concentration from 1 % to 2 %, as a higher number of polymeric chains is available for the crosslinking process [68]. The composition of the media and in particular ionic content was important in the definition of the process kinetic. The faster crosslinking kinetic was found for hydrogels made in DMEM, where bivalent ions are present. This effect was predominant in case of alginate 1 %, affecting gel point and yield stress (Table 1), while the effect of 2 % alginate content shielded these changes induced by culture media composition. Independently of the culture medium used, it is worthy to notice that the viscoelastic properties of I-Bac3Gels resulted to be comparable with the range reported for the physiological loose intestinal mucus layer (*i.e.*, 2–200 Pa) (Figs. 1 and 2) and other *in vitro* mucus model that optimized in terms of viscoelasticity for static drug delivery studies (*i.e.*, 0.2–70 Pa) [62].

Even though viscoelasticity is fundamental in the definition of the bacteria behaviours, the modelling of physiological viscoelastic properties is not sufficient to engineer a complete bioinspired intestinal mucus model. Recently, viscosity, permeability and flow of the mucus model of the intestinal mucus were strongly highlighted as key features [69]. Indeed, the mucus mesh size of the polymer network, which is defined as the distance between two crosslinking points, defines diffusion of oxygen, nutrients and other molecules, impacting on the bacteria distribution and motion [46,70–73]. Despite these evidences, few data are available for the characterization of microstructural parameters in the available intestinal mucus model (*e.g.*, particle tracking and

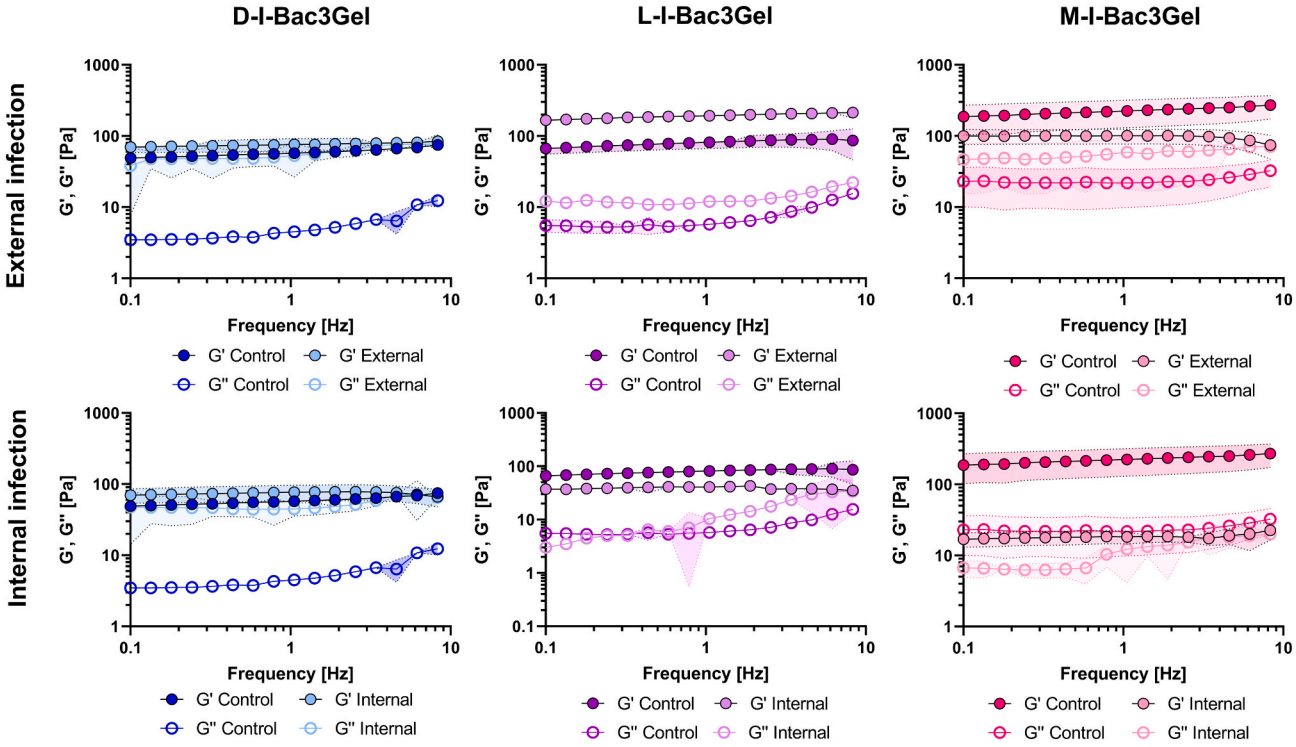

Fig. 8. Frequency spectra of the viscoelastic properties (G' and G'') of D-, L- and M-I-Bac3Gel 1 % obtained with external and internal infection.

porosity) and they are not focused on the polymeric network analysis (*i.e.*, mesh size) [44–46,61]. In the case of the *in vivo* mucus mesh size, the data available in literature are usually obtained by AFM and Multiple Particle Tracking analysis, which showed a polymeric mesh distributed between 20 and 500 nm with a peak around 30 nm [74,75].

In this study, the I-Bac3Gel mesh size was estimated from the shear modulus (G_∞) by fitting frequency sweep data according to the Generalized Maxwell Model [26,52,53]. Even under a microstructural point of view, I-Bac3Gel showed similar ξ to the physiological mucus, independently from the medium used (from 25 ± 5 nm to 42 ± 14 nm, Fig. 5). The G_∞ and ξ resulted to be directly and inversely proportional to the I-Bac3Gels viscoelastic properties, respectively, in coherence with both theory (Eq. (6)) and other studies on alginate hydrogels [76,77].

The control over the composition of the I-Bac3Gels modulated the bacteria organization while maintaining the comparable viability (Figs. 6 and 7). Indeed, the I-Bac3Gels exhibited homogeneous distribution of bacteria along the section independently from the medium type. This is qualitatively similar to *in vivo* animal studies, where it was demonstrated that *E. coli* is equally distributed in the whole loose mucus layer [78,79]. Interestingly, the behaviour of *E. coli* was dependent on the type of medium used. In particular, the confocal microscopy of I-Bac3Gel obtained with Luria Bertani broth showed chain-*like E. coli* aggregation.

LB broth was previously described to promote biofilm cellular chains formation when enriched with glucose, proline and thiamine [80]. The mechanism behind this peculiar behaviour is not fully explained. However, it was related to the presence of specific self-associating autotransporter (SAAT) protein at the bacteria body extremities, whose expression is deeply influenced by the medium composition [51,80,81]. Similarly to I-Bac3Gels obtained with DMEM, the aggregation of bacteria in I-Bac3Gels with LB was more pronounced in case of external infection, where the *E. coli* communication and motion was facilitated. This behaviour is related to the different environments that *E. coli* faces during infection of the models [82,83]. In case of external infection, a collective motion from the liquid phase to the bulk of the hydrogel lead to aggregation, resulting in higher dimension clusters. In case of internal infection, the rapid formation of the alginate networks (Table 1) hampered the bacterial communication and motion, which maintained a homogeneous distribution in the I-Bac3Gels without forming clusters but only small-sized aggregates. These findings are coherent with another study on the *E. coli* aggregation in PEG matrices, where a higher motility degree was found to enhance the clustering process inside the hydrogels [83].

Similarly to what happens *in vivo*, the effect of the mucus features on bacterial behaviour is reflected by an effect of *E. coli* on the mucus properties. Indeed, the I-Bac3Gels internally and externally infected showed three different viscoelastic responses (Fig. 8). A common trend cannot be identified and there is not an univocal effect recognised in other studies characterising the viscoelasticity of infected matrices with reference to culture time and medium composition [84,85]. For example, the presence of *H. pylori* increased the G'' of reconstituted porcine gastric mucus as also occurring in the case of D-I-Bac3Gels infected with *E. coli* [19]. Besides, a G' decrease like in case of M-I-Bac3Gels was also found in literature for *S. aureus* and L. *casei* infections of tryptic soy broth and *k*-carrageenan/locust beam gum beads, respectively [67,68]. The differences in terms of bacterial strains, culture conditions, methods of analysis and type of matrices make these results difficult to be robustly compared. However, taken together, these evidences supported the importance of investigating the influence of bacteria on the matrix used for culture, especially in case of bioinspired substrates.

The maintenance of the optimized viscoelastic properties and microstructure downstream a dynamic stimulation is an essential feature for the application of I-Bac3Gels into advanced microfluidic systems. For this reason, the suitability for dynamic processes was *a priori* investigated theoretically by *ad hoc* rheological characterization and then corroborated experimentally. The power law index and yield stress (Table 1 and Fig. 3) suggested *a priori* the possibility for the I-Bac3Gels to be extruded by using low-magnitude stresses. The capability of I-Bac3gels of being extruded without damage was confirmed *a posteriori*, evaluating the viscoelastic properties and mesh sizes after experimental extrusion (Figs. 4 and 5).

As anticipated by the rheological characterization, the I-Bac3Gels preserved the optimized properties moving from a static to a dynamic condition. Indeed, the dynamic stimulation did not influence the I-Bac3Gels G' and G'' for all the composition considered, except for D-I-Bac3Gels 1 % (Fig. 4). In this case, the increasing viscoelastic properties may be related to an induced orientation of alginate chains during the extrusion at the highest flow rate [69,70]. When a model with higher viscoelastic properties is considered (such as L- and M-I-Bac3Gels), a stiffer polymeric network is present and a lower tendency towards chains orientation is observed [71].

One of the main limitations of the current dynamic bacterial cultures (*e.g.*, gut-on-chip) is the need of medium refresh to avoid bacterial death or overgrowth onto the static 3D matrices. The use of fermenters or other independent sources of medium may guarantee automatic refresh [89,90]. However, the presence of fermenters increases greatly the complexity of the set-up and can be only partially integrated with the needs of 3D matrices, of which there are only a few examples in the literature [74,75]. Differently from these systems, I-Bac3Gels is as a 3D stand-alone tool, which do not require medium refresh up to 24 h. This feature was *per se* observed in static condition (Fig. 6 B), as *E. coli* growth was maintained without the need of medium refresh and further appreciated in the dynamic culture (Fig. 6 C).

The I-Bac3Gels with the minimum concentration of alginate (1 %, *w/v*) was selected as matrix for the dynamic culture of bacterial performed at the maximum flow rate that does not imply significant viscoelastic changes (*i.e.*, 1 μL/min). As the internal gelation imposes to start the dynamic stimulation immediately after preparation, the power law index and the yield stress of the I-Bac3Gels were estimated in a time point of the gelation process that was comparable to time needed for the culture (5 h). Again, rheology indicated the capability of I-Bac3Gel to be extruded without changes in its properties. Indeed, the high extrudability gained thank to low shear resistance (S.I. Fig. 2) found during the *a priori* characterization was corroborated with the experimental evidence of G' and G'' maintenance after extrusion (S.I. Fig. 3). These results confirmed the possibility to combine the 3D culture with the motion, while retaining the physiological-*like* viscoelastic properties (*i.e.*, 2–200 Pa) [26]. These advantages did not affect the bacteria behaviour, as the *E. coli* concentration was found comparable after the dynamic stimulation with the static controls and the culture in suspension (Fig. 6 C). The designed I-Bac3Gels represent a first evidence of an *in vitro* mucus model for bacterial growth that combines bioinspired viscoelastic properties, physiological 3D architecture and dynamic motion in the same moment.

5. Conclusion

Some aspects of engineering models to study the micromechanical features of the intestinal loose mucus layer and how bacteria affect the human body and *vice versa* were faced. Other remains open.

We addressed the possibility to produce a model which can be adapted to different culture conditions by tuning the composition with different cell and bacteria culture media. The different environments shaped the bacteria behaviour. Symmetrically, bacteria altered in different ways the distinct environments. The models can be moved through extrusion in a standalone configuration without medium refresh, while retaining the viscoelastic properties of loose layer and its mesh size, which is relevant for the filtering and barrier function of mucus. The rheological characterization was used as a valid tool to investigate the dynamic process.

Co-cultures of other bacteria strains and microbiota communities are the next steps in the investigation of the of the model suitability as substrate for the 3D dynamic culture of bacteria. In the present work, other aspects rather than chemical similarity were prioritized, such as biosimilar microstructure, rheology and suitability for dynamic application, while the use of standard bacterial and cellular culture media were used to evaluate the effect of chemistry over bacteria cultures. This do not neglect the possibility of engineer the model for future applications of interest, where specific medium and additives, including mucins, can be further added to enrich the culture media here proposed or used to develop *ad hoc*, specific, media.

This work opens to the possibility of exploiting the models in a wide set of static and dynamic applications, including 3D culture of gut microbiota and further optimisation of the gut-on-chip systems to investigate the bacterium-bacterium and bacterium-host cell communication. The possibility to control a priory the rheological application put the basis to develop *ad hoc* models, including the characteristic of pathological scenarios.

CRediT authorship contribution statement

L.S. and P·P. designed the study with the contribution of S·V.; L.S and M.M collected the data and performed data analysis; L.S, A.Z and M.M. performed the biological tests with the supervision of L.V.; FBV conceived and designed the rheological analysis; L.S, P.P., F.B.V., M.M. followed and discussed the ongoing results. L.S. wrote the paper with the contribution of M.M. under the supervision of P.P; S.V, L.V. P.P. and F.B. V. contributed to funding acquisition; all authors revised the paper and approved the submission.

Declaration of competing interest

P.Petrini, S. Visentin and L. Visai are co-founders of Bac3Gel L.t.d. This research activity contributed to set the basis for the successive Bac3Gel Spinoff foundation. Bac3Gel® is now a registered trademark.

Acknowledgements

This work was performed thanks to a grant of the Italian Ministry of Education, University and Research (MIUR) to the Department of Molecular Medicine of the University of Pavia under the initiative “Dipartimenti di Eccellenza (2018–2022)”. P·P. and A.Z. are grateful to “Switch to Product 2018” Innovation program by PoliHub, the Technology Transfer Office at Politecnico di Milano, and Officine Innovazione at Deloitte for supporting of A.Z. stage.

We are grateful to P. Vaghi (Centro Grandi Strumenti: https://cgs.unipv.it/eng/?page_id=84, University of Pavia, Pavia, Italy) for her technical assistance in the CLSM.

Appendix A. Supplementary data

Supplementary data to this article can be found online at https://doi.org/10.1016/j.bioadv.2022.213022.

References

[1] M.E.V. Johansson, H. Sjövall, G.C. Hansson, The gastrointestinal mucus system in health and disease, Nat. Rev. Gastroenterol. Hepatol. 10 (6) (2013) 352–361.
[2] E. Thursby, N. Juge, Introduction to the human gut microbiota, Biochem. J. 474 (11) (2017) 1823–1836.
[3] F. Bäckhed, R.E. Ley, J.L. Sonnenburg, D.A. Peterson, J.I. Gordon, Host-bacterial mutualism in the human intestine, Science (80-.) 307 (5717) (2005) 1915–1920.
[4] J. Dicksved, O. Schreiber, B. Willing, J. Petersson, S. Rang, M. Phillipson, L. Holm, S. Roos, Lactobacillus reuteri maintains a functional mucosal barrier during DSS treatment despite mucus layer dysfunction, PLoS One 7 (9) (2012) 3–10.
[5] M.E.V. Johansson, M. Phillipson, J. Petersson, A. Velcich, L. Holm, G.C. Hansson, J. Petersson, A. Velcich, L. Holm, G.C. Hansson, D. Ambort, M.E. Johansson, J. K. Gustafsson, H.E. Nilsson, A. Ermund, B.R. Johansson, P.J. Koeck, H. Hebert, G. C. Hansson, A. Velcich, W. Yang, J. Heyer, A. Fragale, C. Nicholas, S. Viani, R. Kucherlapati, M. Lipkin, K. Yang, L. Augenlicht, S. Rakoff-Nahoum, J. Paglino, F. Eslami-Varzaneh, S. Edberg, R. Medzhitov, A.L. Frantz, E.W. Rogier, C.R. Weber, L. Shen, D.A. Cohen, L.A. Fenton, M.E. Bruno, C.S. Kaetzel, M. Lamkanfi, V. M. Dixit, E. Elinav, T. Strowig, A.L. Kau, J. Henao-Mejia, C.A. Thaiss, C.J. Booth, D. R. Peaper, J. Bertin, S.C. Eisenbarth, J.I. Gordon, R.A. Flavell, M.E.V. Johansson, K. A. Knoop, K.G. McDonald, S. McCrate, J.R. McDole, R.D. Newberry, M. Wlodarska, C.A. Thaiss, R. Nowarski, J. Henao-Mejia, J.P. Zhang, E.M. Brown, G. Frankel, M. Levy, M.N. Katz, W.M. Philbrick, E. Elinav, B.B. Finlay, R.A. Flavell, D.R. Halm, S.T. Halm, J.K. Gustafsson, R. Zhou, A. Tardivel, B. Thorens, I. Choi, J. Tschopp, F. Bauernfeind, E. Bartok, A. Rieger, L. Franchi, G. Núñez, V. Hornung, R.

D. Specian, M.R. Neutra, M.E.V. Johansson, J.K. Gustafsson, K.E. Sjöberg, J. Petersson, L. Holm, H. Sjövall, G.C. Hansson, H.E. Jakobsson, A.M. Rodríguez-Piñeiro, A. Schütte, A. Ermund, P. Boysen, M. Bemark, F. Sommer, F. Bäckhed, G. C. Hansson, M.E. Johansson, M.E.V. Johansson, J.K. Gustafsson, J. Holmén-Larsson, K.S. Jabbar, L. Xia, H. Xu, F.K. Ghishan, F.A. Carvalho, A.T. Gewirtz, H. Sjövall, G.C. Hansson, K.S.B. Bergstrom, V. Kissoon-Singh, D.L. Gibson, C. Ma, M. Montero, H.P. Sham, N. Ryz, T. Huang, A. Velcich, B.B. Finlay, K. Chadee, B. A. Vallance, J.R. McDole, L.W. Wheeler, K.G. McDonald, B. Wang, V. Konjufca, K. A. Knoop, R.D. Newberry, M.J. Miller, P.C. Colony, R.D. Specian, A. Panday, M. K. Sahoo, D. Osorio, S. Batra, K.K. Patel, H. Miyoshi, W.L. Beatty, R.D. Head, N. P. Malvin, K. Cadwell, J.L. Guan, T. Saitoh, S. Akira, P.O. Seglen, M.C. Dinauer, H. W. Virgin, T.S. Stappenbeck, M.E. Sellin, A.A. Müller, B. Felmy, T. Dolowschiak, M. Diard, A. Tardivel, K.M. Maslowski, W.D. Hardt, L.A. Knodler, S.M. Crowley, H. P. Sham, H. Yang, M. Wrande, C. Ma, R.K. Ernst, O. Steele-Mortimer, J. Celli, B. A. Vallance, D. Demon, A. Kuchmiy, A. Fossoul, Q. Zhu, T.D. Kanneganti, M. Lamkanfi, E.G. Zoetendal, H.G. Heilig, E.S. Klaassens, C.C. Booijink, M. Kleerebezem, H. Smidt, W.M. de Vos, The inner of the two Muc2 mucin-dependent mucus layers in colon is devoid of bacteria, PNAS 105 (39) (2008) 15064–15069.

[6] R. Bansil, B.S. Turner, The biology of mucus: composition, synthesis and organization, Adv. Drug Deliv. Rev. 124 (2018) 3–15.

[7] C.A. Nickerson, C.M. Ott, J.W. Wilson, R. Ramamurthy, D.L. Pierson, Microbial responses to microgravity and other low-shear environments, Microbiol. Mol. Biol. Rev. 68 (2) (2004) 345–361.

[8] A. Crabbé, B. Pycke, R. Van Houdt, P. Monsieurs, C. Nickerson, N. Leys, P. Cornelis, Response of pseudomonas aeruginosa PAO1 to low shear modelled microgravity involves AlgU regulation, Environ. Microbiol. 12 (6) (2010) 1545–1564.

[9] S.L. Castro, M. Nelman-Gonzalez, C.A. Nickerson, C.M. Ott, Induction of attachment-independent biofilm formation and repression of hfq expression by low-fluid-shear culture of Staphylococcus aureus, Appl. Environ. Microbiol. 77 (18) (2011) 6368–6378.

[10] A. Swidsinski, B.C. Sydora, Y. Doerffel, V. Loening-Baucke, M. Vaneechoutte, M. Lupicki, J. Scholze, H. Lochs, L.A. Dieleman, Viscosity gradient within the mucus layer determines the mucosal barrier function and the spatial organization of the intestinal microbiota, Inflamm. Bowel Dis. 13 (8) (2007) 963–970.

[11] E. Deloose, P. Janssen, I. Depoortere, J. Tack, The migrating motor complex: control mechanisms and its role in health and disease, Nat. Rev. Gastroenterol. Hepatol. 9 (5) (May 2012) 271–285.

[12] Y.F. Dufrêne, A. Persat, Mechanomicrobiology: how bacteria sense and respond to forces, Nat. Rev. Microbiol. 18 (4) (2020) 227–240.

[13] V. Osadchiy, C.R. Martin, E.A. Mayer, Gut microbiome and modulation of CNS function, Compr. Physiol. 10 (1) (2020) 57–72.

[14] S. Macfarlane, J.F. Dillon, Microbial biofilms in the human gastrointestinal tract, J. Appl. Microbiol. 102 (5) (2007) 1187–1196.

[15] K.G. Margolis, J.F. Cryan, E.A. Mayer, The microbiota-gut-brain Axis: from motility to mood, Gastroenterology 160 (5) (2021) 1486–1501.

[16] Y. Obata, Á. Castaño, S. Boeing, A.C. Bon-Frauches, C. Fung, T. Fallesen, M.G. de Agüero, B. Yilmaz, R. Lopes, A. Huseynova, S. Horswell, M.R. Maradana, W. Boesmans, P. Vanden Berghe, A.J. Murray, B. Stockinger, A.J. Macpherson, V. Pachnis, Neuronal programming by microbiota regulates intestinal physiology, Nature 578 (7794) (2020) 284–289.

[17] H.E. Jakobsson, A.M. Rodríguez-Piñeiro, A. Schütte, A. Ermund, P. Boysen, M. Bemark, F. Sommer, F. Bäckhed, G.C. Hansson, M.E. Johansson, The composition of the gut microbiota shapes the colon mucus barrier, EMBO Rep. 16 (2) (2015) 164–177.

[18] A. Sontheimer-Phelps, D.B. Chou, A. Tovaglieri, T.C. Ferrante, T. Duckworth, C. Fadel, V. Frismantas, A.D. Sutherland, S. Jalili-Firoozinezhad, M. Kasendra, E. Stas, J.C. Weaver, C.A. Richmond, O. Levy, R. Prantil-Baun, D.T. Breault, D. E. Ingber, Human colon-on-a-Chip enables continuous in vitro analysis of colon mucus layer accumulation and physiology, Cmgh 9 (3) (2020) 507–526.

[19] R. Bansil, J.P. Celli, J.M. Hardcastle, B.S. Turner, The influence of mucus microstructure and rheology in helicobacter pylori infection, Front. Immunol. 4 (OCT) (2013) 1–12.

[20] J.P. Celli, B.S. Turner, N.H. Afdhal, S. Keates, I. Ghiran, C.P. Kelly, R.H. Ewoldt, G. H. McKinley, P. So, S. Erramilli, R. Bansil, Helicobacter pylori moves through mucus by reducing mucin viscoelasticity, Proc. Natl. Acad. Sci. U. S. A. 106 (34) (2009) 14321–14326.

[21] A.P. Corfield, The interaction of the gut microbiota with the mucus barrier in health and disease in human, Microorganisms 6 (3) (2018) 18–26.

[22] R.H. Dosh, A. Essa, N. Jordan-Mahy, C. Sammon, C.L. Le Maitre, Use of hydrogel scaffolds to develop an in vitro 3D culture model of human intestinal epithelium, Acta Biomater. 62 (2017) 128–143.

[23] S. Jalili-Firoozinezhad, F.S. Gazzaniga, E.L. Calamari, D.M. Camacho, C.W. Fadel, A. Bein, B. Swenor, B. Nestor, M.J. Cronce, A. Tovaglieri, O. Levy, K.E. Gregory, D. T. Breault, J.M.S. Cabral, D.L. Kasper, R. Novak, D.E. Ingber, A complex human gut microbiome cultured in an anaerobic intestine-on-a-chip, Nat. Biomed. Eng. 3 (July) (2019).

[24] P. Shah, J.V. Fritz, E. Glaab, M.S. Desai, K. Greenhalgh, A. Frachet, M. Niegowska, M. Estes, C. Jäger, C. Seguin-Devaux, F. Zenhausern, P. Wilmes, A microfluidics-based in vitro model of the gastrointestinal human-microbe interface, Nat. Commun. 7 (May) (2016).

[25] Z. Jia, Z. Guo, C.-T. Yang, C. Prestidge, B. Thierry, 'Mucus-on-Chip': A new tool to study the dynamic penetration of nanoparticulate drug carriers into mucus, Int. J. Pharm. 598 (January) (2021) 120391.

[26] D.P. Pacheco, C.S. Butnarasu, F. Briatico Vangosa, L. Pastorino, L. Visai, S. Visentin, P. Petrini, Disassembling the complexity of mucus barriers to develop a fast screening tool for early drug discovery, J. Mater. Chem. B 7 (32) (2019) 4940–4952.

[27] E.A. Growney Kalaf, R. Flores, J.G. Bledsoe, S.A. Sell, Characterization of slow-gelling alginate hydrogels for intervertebral disc tissue-engineering applications, Mater. Sci. Eng. C 63 (2016) 198–210.

[28] C.E. Campiglio, S.J. Bidarra, L. Draghi, C.C. Barrias, Bottom-up engineering of cell-laden hydrogel microfibrous patch for guided tissue regeneration, Mater. Sci. Eng. C 108 (Mar. 2020).

[29] J. Crisóstomo, A.M. Pereira, S.J. Bidarra, A.C. Gonçalves, P.L. Granja, J.F.J. Coelho, C.C. Barrias, R. Seiça, ECM-enriched alginate hydrogels for bioartificial pancreas: an ideal niche to improve insulin secretion and diabetic glucose profile, J. Appl. Biomater. Funct. Mater. 17 (4) (2019) Oct.

[30] M. Oriano, L. Zorzetto, G. Guagliano, F. Bertoglio, S. van Uden, L. Visai, P. Petrini, The open challenge of in vitro modeling complex and multi-microbial communities in three-dimensional niches, Front. Bioeng. Biotechnol. 8 (October) (2020) 1–17.

[31] S.M. Blevins, M.S. Bronze, Robert koch and the 'golden age' of bacteriology, Int. J. Infect. Dis. 14 (9) (2010) 744–751.

[32] G. Swaminathan, N. Kamyabi, H.E. Carter, A. Rajan, U. Karandikar, Z.K. Criss, N. F. Shroyer, M.J. Robertson, C. Coarfa, C. Huang, T.E. Shannon, M. Tadros, M. K. Estes, A.W. Maresso, K.J. Grande-Allen, Effect of substrate stiffness on human intestinal enteroids' infectivity by enteroaggregative Escherichia coli, Acta Biomater. 132 (2021) 245–259.

[33] S. Gognies, A. Belarbi, Use of a new gelling agent (Eladium©) as an alternative to agar-agar and its adaptation to screen biofilm-forming yeasts, Appl. Microbiol. Biotechnol. 88 (5) (2010) 1095–1102.

[34] J.A. Lichter, M.T. Thompson, M. Delgadillo, T. Nishikawa, M.F. Rubner, K.J. Van Vliet, Erratum: substrata mechanical stiffness can regulate adhesion of viable bacteria (Biomacromolecules (2008) vol 9 (1574–1576)), Biomacromolecules 9 (10) (2008) 2967.

[35] X.D. Wang, R.J. Meier, O.S. Wolfbeis, Fluorescent pH-sensitive nanoparticles in an agarose matrix for imaging of bacterial growth and metabolism, Angew. Chem. Int. Ed. 52 (1) (2013) 406–409.

[36] D. Shungu, M. Valiant, V. Tutlane, GELRITE as an agar substitute in bacteriological media, Appl. Environ. Microbiol. 46 (4) (1983) 840–845.

[37] S.B. Babbar, R. Jain, Xanthan gum: an economical partial substitute for agar in microbial culture media, Curr. Microbiol. 52 (4) (2006) 287–292.

[38] R. Jain, V. Anjaiah, S.B. Babbar, Guar gum: a cheap substitute for agar in microbial culture media, Lett. Appl. Microbiol. 41 (4) (2005) 345–349.

[39] H.H. Tuson, L.D. Renner, D.B. Weibel, Polyacrylamide hydrogels as substrates for studying bacteria, Chem. Commun. 48 (10) (2012) 1595–1597.

[40] A.D. Augst, H.J. Kong, D.J. Mooney, Alginate hydrogels as biomaterials, Macromol. Biosci. 6 (8) (2006) 623–633.

[41] M. Soutto, Z. Chen, A.M. Katsha, J. Romero-Gallo, U.S. Krishna, M.B. Piazuelo, M. K. Washington, R.M. Peek, A. Belkhiri, W.M. El-Rifai, Trefoil factor 1 expression suppresses H elicobacter pylori -induced inflammation in gastric carcinogenesis, Cancer 121 (24) (2015) 4348–4358.

[42] J. Ann Naughton, K. Mariño, B. Dolan, C. Reid, R. Gough, M.E. Gallagher, M. Kilcoyne, J.Q. Gerlach, L. Joshi, P. Rudd, S. Carrington, B. Bourke, M. Clyne, Divergent mechanisms of interaction of helicobacter pylori and campylobacter jejuni with mucus and mucins, Infect. Immun. 81 (8) (2013) 2838–2850.

[43] A. Flannery, J. Gerlach, L. Joshi, M. Kilcoyne, Assessing bacterial interactions using carbohydrate-based microarrays, Microarrays 4 (4) (2015) 690–713.

[44] M. Boegh, S.G. Baldursdóttir, A. Müllertz, H.M. Nielsen, Property profiling of biosimilar mucus in a novel mucus-containing in vitro model for assessment of intestinal drug absorption, Eur. J. Pharm. Biopharm. 87 (2) (2014) 227–235.

[45] B.C. Huck, O. Hartwig, A. Biehl, K. Schwarzkopf, C. Wagner, B. Loretz, X. Murgia, C.M. Lehr, Macro- and microrheological properties of mucus surrogates in comparison to native intestinal and pulmonary mucus, Biomacromolecules 20 (9) (2019) 3504–3512.

[46] A. Sharma, J.-G. Kwak, K.W. Kolewe, J.D. Schiffman, N.S. Forbes, J. Lee, In vitro reconstitution of an intestinal mucus layer shows that cations and pH control the pore structure that regulates its permeability and barrier function, ACS applBio Mater. 3 (5) (2020) 2897–2909.

[47] A. Leimbach, J. Hacker, U. Dobrindt, E. Coli as an all-rounder: the thin line between commensalism and pathogenicity, Assess. Eval. High. Educ. 37 (October) (2013) 3–32.

[48] N. Figueroa-Morales, L. Dominguez-Rubio, T.L. Ott, I.S. Aranson, Mechanical shear controls bacterial penetration in mucus, Sci. Rep. 9 (1) (2019) 1–10.

[49] J. In, J. Foulke-Abel, N.C. Zachos, A.M. Hansen, J.B. Kaper, H.D. Bernstein, M. Halushka, S. Blutt, M.K. Estes, M. Donowitz, O. Kovbasnjuk, Enterohemorrhagic Escherichia coli reduces mucus and intermicrovillar bridges in human stem cell-derived colonoids, Cmgh 2 (1) (2016) 48–62.e3.

[50] A.K. Møller, M.P. Leatham, T. Conway, P.J.M. Nuijten, L.A.M. De Haan, K. A. Krogfelt, P.S. Cohen, An Escherichia coli MG1655 lipopolysaccharide deep-rough core mutant grows and survives in mouse cecal mucus but fails to colonize the mouse large intestine, Infect. Immun. 71 (4) (2003) 2142–2152.

[51] M.E. Mokszycki, M. Leatham-Jensen, J.L. Steffensen, Y. Zhang, K.A. Krogfelt, M. E. Caldwell, T. Conway, P.S. Cohen, A simple in vitro gut model for studying the interaction between Escherichia coli and the intestinal commensal microbiota in cecal mucus, Appl. Environ. Microbiol. 84 (24) (2018) Dec.

[52] L. Sardelli, M. Tunesi, F. Briatico-Vangosa, P. Petrini, 3D-reactive printing of engineered alginate inks, Soft Matter (2021) 37–39.

[53] P. Matricardi, F. Alhaique, T. Coviello, Polysaccharide Hydrogels, 2016.

[54] M.R. Green, J. Sambrook, Transformation of Escherichia coli by electroporation, Cold Spring Harb. Protoc. 2020 (6) (2020) 232–238.

[55] Y. Magariyama, M. Ichiba, K. Nakata, K. Baba, T. Ohtani, S. Kudo, T. Goto, Difference in bacterial motion between forward and backward swimming caused by the wall effect, Biophys. J. 88 (5) (2005) 3648–3658.
[56] J.C. Clemente, L.K. Ursell, L.W. Parfrey, R. Knight, The impact of the gut microbiota on human health: an integrative view, Cell 148 (6) (2012) 1258–1270.
[57] F. Backhed, Host-bacterial mutualism in the human intestine, Science (80-.) 307 (5717) (2005) 1915–1920.
[58] S. Fanaro, R. Chierici, P. Guerrini, V. Vigi, Intestinal microflora in early infancy, Acta Paediatr. Suppl. 91 (1) (2003) 48–55.
[59] L.E. Tailford, E.H. Crost, D. Kavanaugh, N. Juge, Mucin glycan foraging in the human gut microbiome, Front. Genet. 5 (FEB) (2015).
[60] A. Macierzanka, A.R. Mackie, B.H. Bajka, N.M. Rigby, F. Nau, D. Dupont, Transport of particles in intestinal mucus under simulated infant and adult physiological conditions: impact of mucus structure and extracellular DNA, PLoS One 9 (4) (2014) 1–11.
[61] M. Boegh, S.G. Baldursdottir, M.H. Nielsen, A. Müllertz, H.M. Nielsen, Development and rheological profiling of biosimilar mucus, Annu. Trans. Nord. Rheol. Soc. 21 (2013) 233–240.
[62] L. Sardelli, D.P. Pacheco, A. Ziccarelli, M. Tunesi, O. Caspani, A. Fusari, F. Briatico Vangosa, C. Giordano, P. Petrini, Towards bioinspired in vitro models of intestinal mucus, RSC Adv. 9 (28) (2019) 15887–15899.
[63] M. Bonnet, J.C. Lagier, D. Raoult, S. Khelaifia, Bacterial culture through selective and non-selective conditions: the evolution of culture media in clinical microbiology, New Microbes New Infect. 34 (2020).
[64] Y. Zhang, C. An, Y. Zhang, H. Zhang, A.F. Mohammad, Q. Li, W. Liu, F. Shao, J. Sui, C. Ren, K. Sun, F. Cheng, J. Liu, H. Wang, Microfluidic-templating alginate microgels crosslinked by different metal ions as engineered microenvironment to regulate stem cell behavior for osteogenesis, Mater. Sci. Eng. C 131 (July) (2021) 112497.
[65] K. Prasad, A.K. Siddhanta, A.K. Rakshit, A. Bhattacharya, P.K. Ghosh, On the properties of agar gel containing ionic and non-ionic surfactants, Int. J. Biol. Macromol. 35 (3–4) (2005) 135–144.
[66] N. Das, N. Triparthi, S. Basu, C. Bose, S. Maitra, S. Khurana, Progress in the development of gelling agents for improved culturability of microorganisms, Front. Microbiol. 6 (JUN) (2015) 1–7.
[67] T. Tanaka, K. Kawasaki, S. Daimon, W. Kitagawa, K. Yamamoto, H. Tamaki, M. Tanaka, C.H. Nakatsu, Y. Kamagata, A hidden pitfall in the preparation of agar media undermines microorganism cultivability, Appl. Environ. Microbiol. 80 (24) (2014) 7659–7666.
[68] C.K. Kuo, P.X. Ma, Ionically crosslinked alginate hydrogels as scaffolds for tissue engineering: part 1. Structure, gelation rate and mechanical properties, Biomaterials 22 (6) (2001) 511–521.
[69] L. Wright, P. Joyce, T.J. Barnes, C.A. Prestidge, Mimicking the gastrointestinal mucus barrier: laboratory-based approaches to facilitate an enhanced understanding of mucus permeation, ACS Biomater. Sci. Eng. (2021), https://doi.org/10.1021/acsbiomaterials.1c00814.
[70] H. Suhaimi, S. Wang, T. Thornton, D.B. Das, On glucose diffusivity of tissue engineering membranes and scaffolds, Chem. Eng. Sci. 126 (2015) 244–256.
[71] F. Qu, Q. Li, X. Wang, X. Cao, M.H. Zgonis, J.L. Esterhai, V.B. Shenoy, L. Han, R. L. Mauck, Maturation state and matrix microstructure regulate interstitial cell migration in dense connective tissues, Sci. Rep. 8 (1) (2018) 1–13.
[72] B. Borer, R. Tecon, D. Or, Spatial organization of bacterial populations in response to oxygen and carbon counter-gradients in pore networks, Nat. Commun. 9 (1) (Dec. 2018) 769.
[73] J. Luo, J. Zhu, L. Wang, J. Kang, X. Wang, J. Xiong, Co-electrospun nano-/microfibrous composite scaffolds with structural and chemical gradients for bone tissue engineering, Mater. Sci. Eng. C 119 (March 2018) (2021) 111622.
[74] A.N. Round, N.M. Rigby, A. Garcia de la Torre, A. Macierzanka, E.N.C. Mills, A. R. Mackie, Lamellar structures of MUC2-rich mucin: a potential role in governing the barrier and lubricating functions of intestinal mucus, Biomacromolecules 13 (10) (2012) 3253–3261.
[75] H.M. Yildiz, C.A. McKelvey, P.J. Marsac, R.L. Carrier, Size selectivity of intestinal mucus to diffusing particulates is dependent on surface chemistry and exposure to lipids, J. Drug Target. 23 (7–8) (Sep. 2015) 768–774.
[76] G. Kaklamani, D. Cheneler, L.M. Grover, M.J. Adams, J. Bowen, Mechanical properties of alginate hydrogels manufactured using external gelation, J. Mech. Behav. Biomed. Mater. 36 (2014) 135–142.
[77] G. Turco, I. Donati, M. Grassi, G. Marchioli, R. Lapasin, S. Paoletti, Mechanical spectroscopy and relaxometry on alginate hydrogels: a comparative analysis for structural characterization and network mesh size determination, Biomacromolecules 12 (4) (2011) 1272–1282.
[78] M.E.V. Johansson, J.K. Gustafsson, J. Holmen-Larsson, K.S. Jabbar, L. Xia, H. Xu, F. K. Ghishan, F.A. Carvalho, A.T. Gewirtz, H. Sjovall, G.C. Hansson, Bacteria penetrate the normally impenetrable inner colon mucus layer in both murine colitis models and patients with ulcerative colitis, Gut 63 (2) (2014) 281–291.
[79] J.H. Bergström, G.M.H. Birchenough, G. Katona, B.O. Schroeder, A. Schütte, in: Gram-positive Bacteria Are Held at a Distance in the Colon Mucus by the Lectin-like Protein ZG16 113, 2016, pp. 13833–13838, no. 48.
[80] R.M. Vejborg, P. Klemm, Cellular chain formation in Escherichia coli biofilms, Microbiology 155 (5) (2009) 1407–1417.
[81] U. Frömmel, A. Böhm, J. Nitschke, J. Weinreich, J. Groß, S. Rödiger, T. Wex, H. Ansorge, O. Zinke, C. Schröder, D. Roggenbuck, P. Schierack, Adhesion patterns of commensal and pathogenic Escherichia coli from humans and wild animals on human and porcine epithelial cell lines, Gut Pathog. 5 (1) (2013).
[82] G. Dorken, G.P. Ferguson, C.E. French, W.C.K. Poon, Aggregation by depletion attraction in cultures of bacteria producing exopolysaccharide, J. R. Soc. Interface 9 (77) (Dec. 2012) 3490–3502.
[83] M.K. Porter, A. Preska Steinberg, R.F. Ismagilov, Interplay of motility and polymer-driven depletion forces in the initial stages of bacterial aggregation, Soft Matter 15 (35) (2019) 7071–7079.
[84] P. Patrício, P.L. Almeida, R. Portela, R.G. Sobral, I.R. Grilo, T. Cidade, C.R. Leal, Living bacteria rheology: Population growth, aggregation patterns, and collective behavior under different shear flows, Phys. Rev. E - Stat. Nonlinear, Soft Matter Phys. 90 (2) (2014).
[85] C. Lacroix, C. Paquin, J.P. Arnaud, Batch fermentation with entrapped growing cells of lactobacillus casei - optimization of the rheological properties of the entrapment gel matrix, Appl. Microbiol. Biotechnol. 32 (4) (1990) 403–408.
[89] D. Herbert, R. Elsworth, R.C. Telling, The continuous culture of bacteria; a theoretical and experimental study, J. Gen. Microbiol. 14 (3) (Jul. 1956) 601–622.
[90] L. Sardelli, S. Perottoni, M. Tunesi, L. Boeri, F. Fusco, P. Petrini, D. Albani, C. Giordano, Technological tools and strategies for culturing human gut microbiota in engineered in vitro models, Biotechnol. Bioeng. 118 (8) (Aug. 2021) 2886–2905.

Further reading

[92] A. Groisman, C. Lobo, H. Cho, J.K. Campbell, Y.S. Dufour, A.M. Stevens, A. Levchenko, A microfluidic chemostat for experiments with bacterial and yeast cells, Nat. Methods 2 (9) (2005) 685–689.